Multiscale tribo-mechanical behavior of natural fiber composites

1. **Faissal Chegdani** *

   - Arts et Metiers Institute of Technology, MSMP, HESAM Université, F-51006, Châlons-en-Champagne, France.

   Email: faissal.chegdani@ensam.eu

2. **Mohamed El Mansori**

   - Arts et Metiers Institute of Technology, MSMP, HESAM Université, F-51006, Châlons-en-Champagne, France
   - Texas A&M Engineering Experiment Station, Institute for Manufacturing Systems, College Station, TX 77843, USA

   Email: mohamed.elmansori@ensam.eu

ABSTRACT: (50-100 words)

The use of natural fibers in composite industry requires a deep understanding of their complex mechanical behavior related to their multiscale cellulosic structure. This chapter aims to investigate the tribo-mechanical properties of flax fiber reinforced polypropylene composites using nanoindentation and scratch-test techniques in order to analyze each composite phase separately. Unlike the polymer matrix, the tribo-mechanical behavior of flax fibers shows a strong scale effect that is controlled by the chemical composition of the natural fiber. This specific comportment is also impacted by the temperature. The outcomes of this investigation should be considered for the design of these eco-friendly materials.

KEYWORDS: (10-15 keywords)

Natural fiber composites; Cellulose microfibrils; Hemicellulose; Lignin; Pectin; Atomic Force Microscopy; Rigid Probe Microscopy; Elastic Modulus; Friction Coefficient; Temperature.

* Corresponding author

1. Introduction

Natural fiber composites (NFC) are arousing the interest of automotive and aerospace industry thanks to many economic, ecological, and technical benefits that natural fibers provide to the composite applications (Dittenber and GangaRao, 2012; Faruk et al., 2012; Mastura et al., 2018; Ramesh et al., 2017; Yan et al., 2014). Therefore, many research works have addressed the manufacturing processes of these ecofriendly materials to investigate the possibility to substitute glass fiber composites in the composite industry (Bos et al., 2006; Goutianos et al., 2006; Jiang et al., 2017; Shah, 2013; Shalwan and Yousif, 2013).

Machining processes, which are unavoidable operations for industrial parts made with long fiber composites, were also investigated to understand the cutting behavior of natural fibers and optimize the machined surface quality of NFC materials (Chegdani et al., 2018a, 2016; F. Chegdani et al., 2015; Faissal Chegdani et al., 2015; Chegdani and El Mansori, 2019, 2018; Chegdani and Mansori, 2018; Lotfi et al., 2019; Nassar et al., 2017; Rajmohan et al., 2019; Roy Choudhury et al., 2018; Vinayagamoorthy and Rajmohan, 2018). It has been shown that the machinability of NFC is highly sensitive to the small variations of material and process parameters (Refer to Chapter 7.8 for further details). The specific cutting behavior of natural fibers is caused by their multiscale complex structure that differs from nanoscale to macroscale (Baley, 2002; Charlet et al., 2007; Marrot et al., 2013). In order to control the machinability of NFC materials, the tribomechanical behavior of natural fibers within the composite should be investigated and understood at each scale level of the natural fibrous structure.

This chapter proposes a multiscale tribomechanical study on flax fiber reinforced polypropylene composites. The aim is to explore both the mechanical and the tribological responses of falx fibers and polypropylene separately and at different

contact scale levels. This will give to the reader an advanced knowledge about the scale effect on the tribomechanical behavior of natural fibers within the composite materials.

2. Multiscale structure of natural fibrous reinforcement in composites

Figure 1 illustrates the multiscale structure of NFC materials from macroscale to nanoscale. The macroscopic scale covers the overall composite structure that contains the natural fibrous reinforcement and the polymer matrix (Figure 1(a)). The mesoscopic scale distinguishes the technical fiber that includes some elementary fibers gathered together naturally with pectic interfaces (Figure 1(b)). At microscale, each elementary fiber is structured with a stacking of cellulosic cell walls (Figure 1(c)). The important cell wall is S2 that covers the main fiber volume and controls the fiber properties (Baley, 2002). As shown in Figure 1(d), the cell wall S2 is itself a composite material at nanoscale with cellulose microfibrils embedded in natural amorphous polymers of hemicellulose, lignin, and pectin (Baley, 2002; Charlet et al., 2007). Cellulose microfibrils are oriented toward the fiber axis with and angle "θ" called microfibrillar angle.

Figure 1 demonstrates that NFC materials have different compositions that vary by changing the scale level. This finding is should be considered to investigate the behavior of NFC during high tribomechanical solicitations such as machining. The next sections will address the contact scale effect on the tribomechanical reponse of NFC.

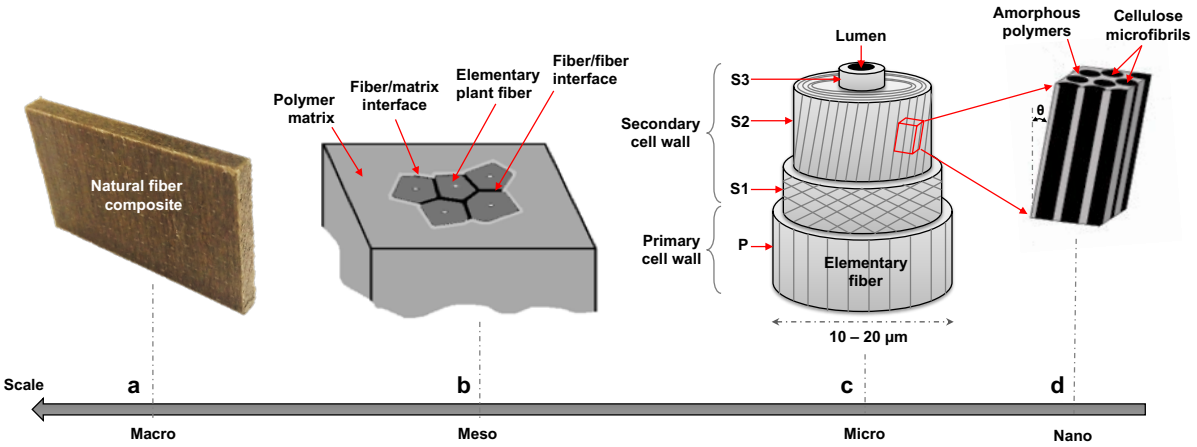

Figure 1: Multiscale structure of natural fiber composites from macroscale to nanoscale

3. Experimental procedure

3.1. NFC samples

NFC samples used in this study are composed of unidirectional flax fibers as reinforcement and polypropylene (PP) as polymer matrix as shown in Figure 2(a). The worksurface is perpendicular to the fiber orientation in order to perform the tribomechanical experiments on the cross-sections of flax fibers as shown in Figure 2(b). It can be seen that flax fibers present a high variability in terms of shape and diameter which a high variability on their mechanical properties obtained from literature by mechanical tensile tests (Dittenber and GangaRao, 2012).

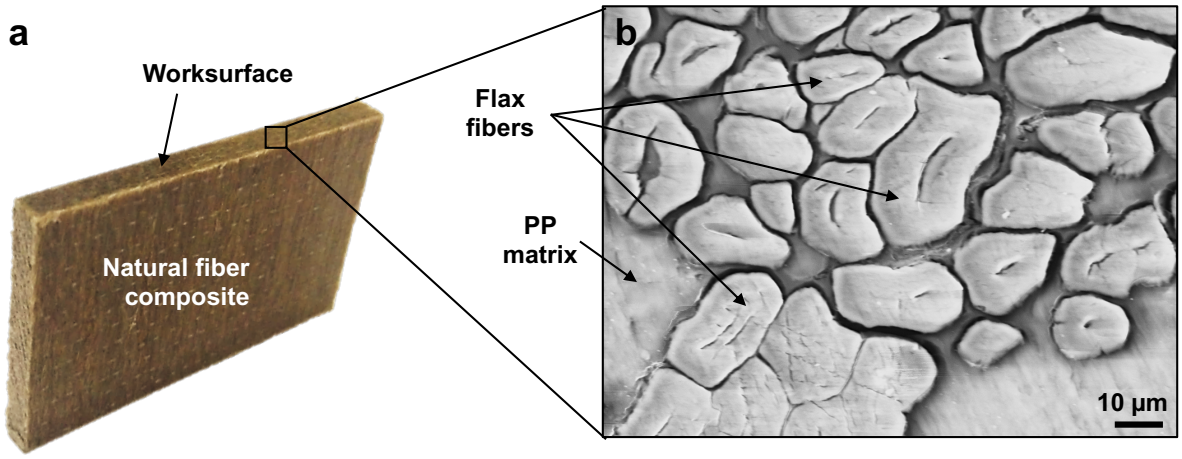

Figure 2: (a) photographic image of unidirectional flax fiber composite sample. (b) SEM image of the worksurface of unidirectional flax fiber composite sample

3.2. Tribomechanical tests approach

The tribomechanical method used in this study is based on nanoindentation and scratch-test experiments. The choice of these two tribomechanical techniques is justified by the fact that both mechanical and tribological experiments should be performed on flax fibers and PP matrix separately in order to reveal the tribomechanical response of each composite phase.

Nanomechanical characterization is used to measure and evaluate numerous mechanical properties of materials, including modulus, hardness, fracture toughness, wear resistance and friction coefficient. Nanomechanical characterization, as well as visualization of surface topography, provides crucial information concerning the performance of materials. Nanoindentation is commonly used to characterize the local stiffness of materials by determining the elastic modulus and hardness. On the other hand, acquiring quantitative force and displacement data in the lateral direction leads to the quantification of friction coefficient, scratch resistance and wear parameters.

Two different techniques for nanoindentation and scratch-test have emerged. These are Atomic Force Microscopy (AFM) and Rigid Probe Microscopy (RPM) as shown in

Figure 3. Nanoindentation and nanoscratching with AFM technique are based on the cantilever deflection when the tip indenter is in contact with the material (Figure 3(a)). The cantilever deflection is measured using a laser sensor. This characterization method requires small contact areas in order to avoid the inaccuracy of measurements caused by the own deflection of the cantilever. Therefore, smaller tips indenter radii (r < 100 nm) can be used to indent the sample surface, and it is possible to produce low force indentations over the desired region with well-controlled position accuracy (Monclus et al., 2010). For the RPM technique, the tip indenter is directly related to a rigid probe that is normal to the surface as shown in Figure 3(b). This configuration avoids the cantilevered motion and allows the use of higher loadings and higher tip indenter radii comparing to the AFM technique.

The AFM method has been used in this study with “Dimension Edge™” instrument from “Bruker©”. Berkovich diamond tip indenter is considered with a small tip radius (r = 40 nm). The tip indenter is related to a steel cantilever that has a spring constant of 450 N/m.

The RPM technique has been performed with two instruments:

- The commercial tribomechanical instrument “Nanoindenter XP” from “MTS Nano Instruments©” equipped with a Berkovich diamond tip indenter that has a tip radius of ~ 400 nm.
- The commercial tribomechanical instrument “TI-950” from “Hysitron©”. Two tip indenters have been tested: Berkovich diamond tip indenter and Berkovich Sapphire tip indenter that have a tip radius of 100 nm and 150 nm, respectively.

The aim of this instrument’s choice is to investigates a large range of tip indenter radii and evaluate the effect of the geometrical contact scale.

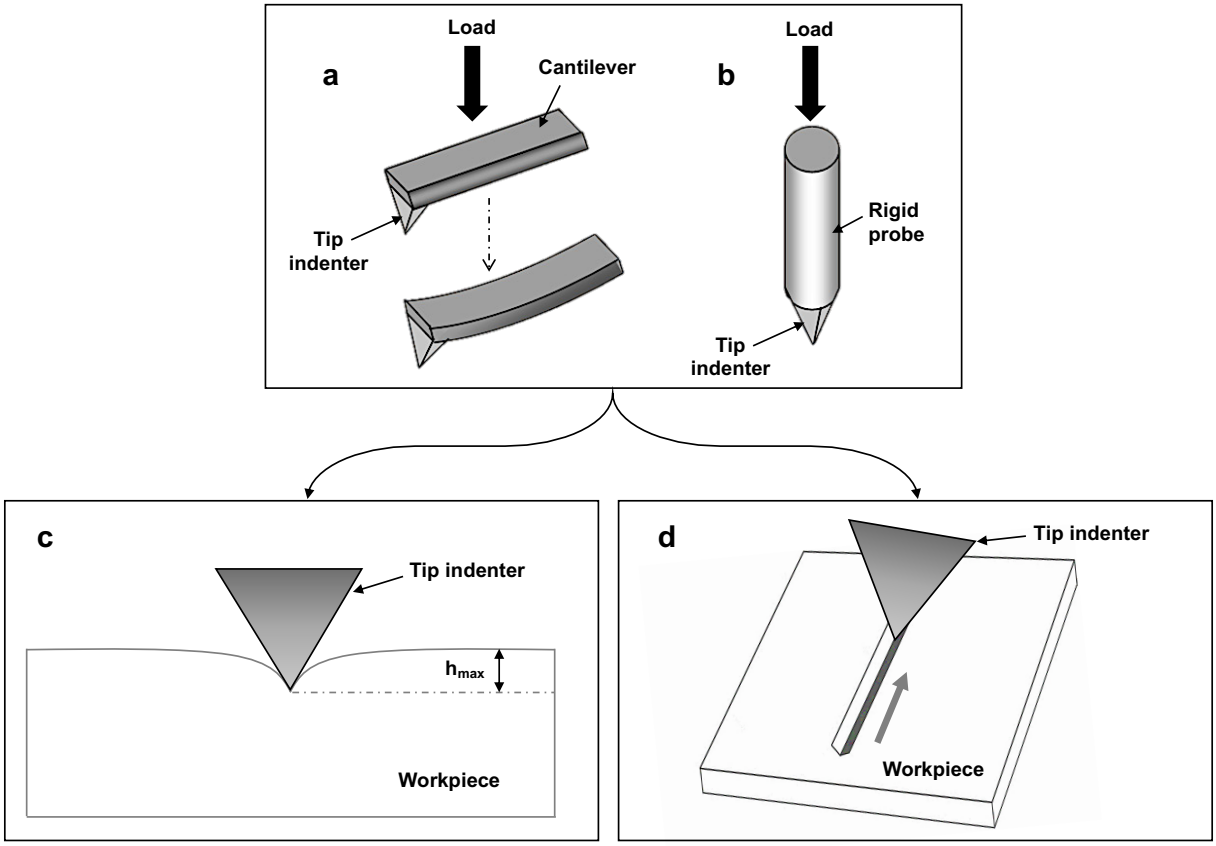

Figure 3: Schematic illustration of (a) AFM indenter, (b) RPM indenter, (c) Nanoindentation technique, and (d) Scratch-test technique

3.2.1. Nanoindentation analysis

Nanoindentation method involves the normal contact of an indenter on the worksurface and its penetration in this surface to a specified load or depth as illustrated in Figure 4(a) (Bourmaud and Pimbert, 2008). The load is measured as a function of penetration depth as shown in Figure 4(b). From this load–penetration curve, the pertinent parameters for the analysis are the maximum displacement (h_{max}), the maximum load on the sample (F_{max}), and the contact stiffness (S) which is the slope of the tangent line to the unloading curve at the maximum loading point (see Figure 4(b)).

In the case of Berkovich tip indenter, the model of Oliver & Pharr (Oliver and Pharr, 1992) is generally used to calculate the elastic modulus of each material using the parameters extracted from load–penetration curve of nanoindentation. This model

assumes the elastic behavior as the basis foundation of this calculation procedure (Doerner and Nix, 1986; Oliver and Pharr, 1992). The Oliver & Pharr method consists on computing the contact depth (h_c) which is dependent on the material deformation and the tip shape as shown in Figure 4(a). h_c can be calculated using the Eq (1). ε is a constant related to the tip geometry (0.72 for Berkovich tip (Bourmaud and Pimbert, 2008)). The projected contact area (A) can be calculated using the Eq (2). Then, the reduced elastic modulus is obtained using the Eq (3) where β is a constant related to the tip geometry (1.034 for Berkovich tip (Bourmaud and Pimbert, 2008)). Finally, the elastic modulus of the indented material can be calculated with the Eq (4) where E_i and ν_i are respectively the elastic modulus and the Poisson coefficient of the tip indenter. ν is the Poisson coefficient of the indented material.

$$h_c = h_{max} - \varepsilon \frac{F_{max}}{S} \tag{1}$$

$$A = 24.56 \times h_c^2 \tag{2}$$

$$E_r = \frac{S\sqrt{\pi}}{2\beta\sqrt{A}} \tag{3}$$

$$\frac{1}{E_r} = \frac{(1-\nu^2)}{E} + \frac{(1-\nu_i^2)}{E_i} \tag{4}$$

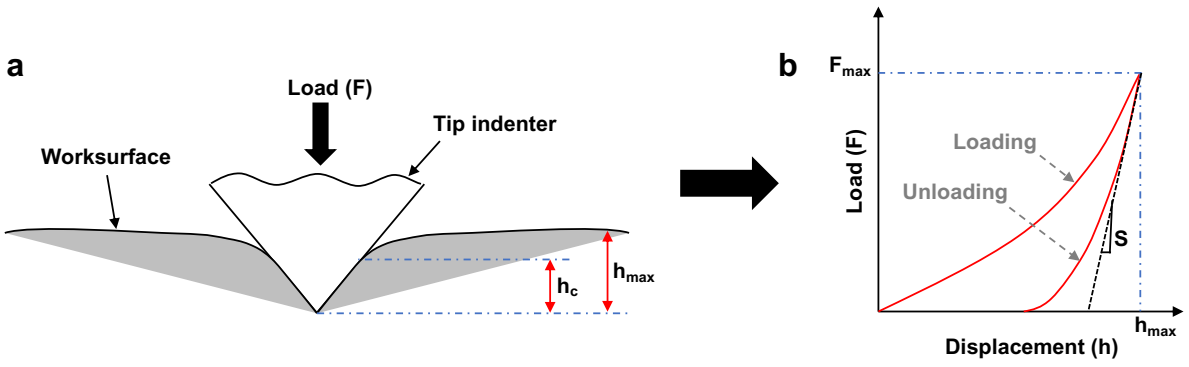

Figure 4: (a) Schematic illustration of the contact between the tip indenter and the worksurface. (b) Typical load/displacement curve generated by nanoindentation tests

3.2.2. Scratch-test analysis

Scratch-test method involves the sliding contact of an indenter on the worksurface and the resistance of this surface to the sliding motion. Indeed, the tip indenter slides on the worksurface with specific load, speed, and length (Figure 3(d)). The in-situ normal and lateral forces are measured and the dynamic friction coefficient (μ_D) is calculated as the ratio between the lateral force and the normal force. In this study, the considered scratching length is 10 µm in order to work on elementary flax fibers and PP matrix separately. μ_D is evaluated in function of sliding speed and load.

4. Scale effect on the tribo-mechanical response of natural fiber composites

4.1. Multiscale mechanical response of natural fiber composites

As explained in section 3.2, the mechanical characterization of NFC is realized on elementary fibers and polymer matrix separately. The mechanical response of flax fibers and PP matrix has been first performed by nanoindentation using the AFM method with diamond Berkovich indenter (r = 40 nm) and am applied load of 500 µN (Chegdani et al., 2017).

Figure 5 presents the indentation traces and the corresponding elastic modulus values for flax fibers and PP matrix. Figure 5(a) and Figure 5(c) show that nanoindentation technique is able to target flax fibers and PP matrix separately. The elastic modulus of PP matrix is more affected by the contact depth than that of flax fibers. With the same applied load, flax fiber generates contact depths between 170 nm and 210 nm (Figure 5(b)), while PP matrix generates contact depths between 70 nm and 160 nm (Figure

5(d)). Consequently, the elastic modulus of PP matrix (~ 1 – 2 GPa) is higher than that of flax fibers (~ 0.7 – 1 GPa) at the same applied load.

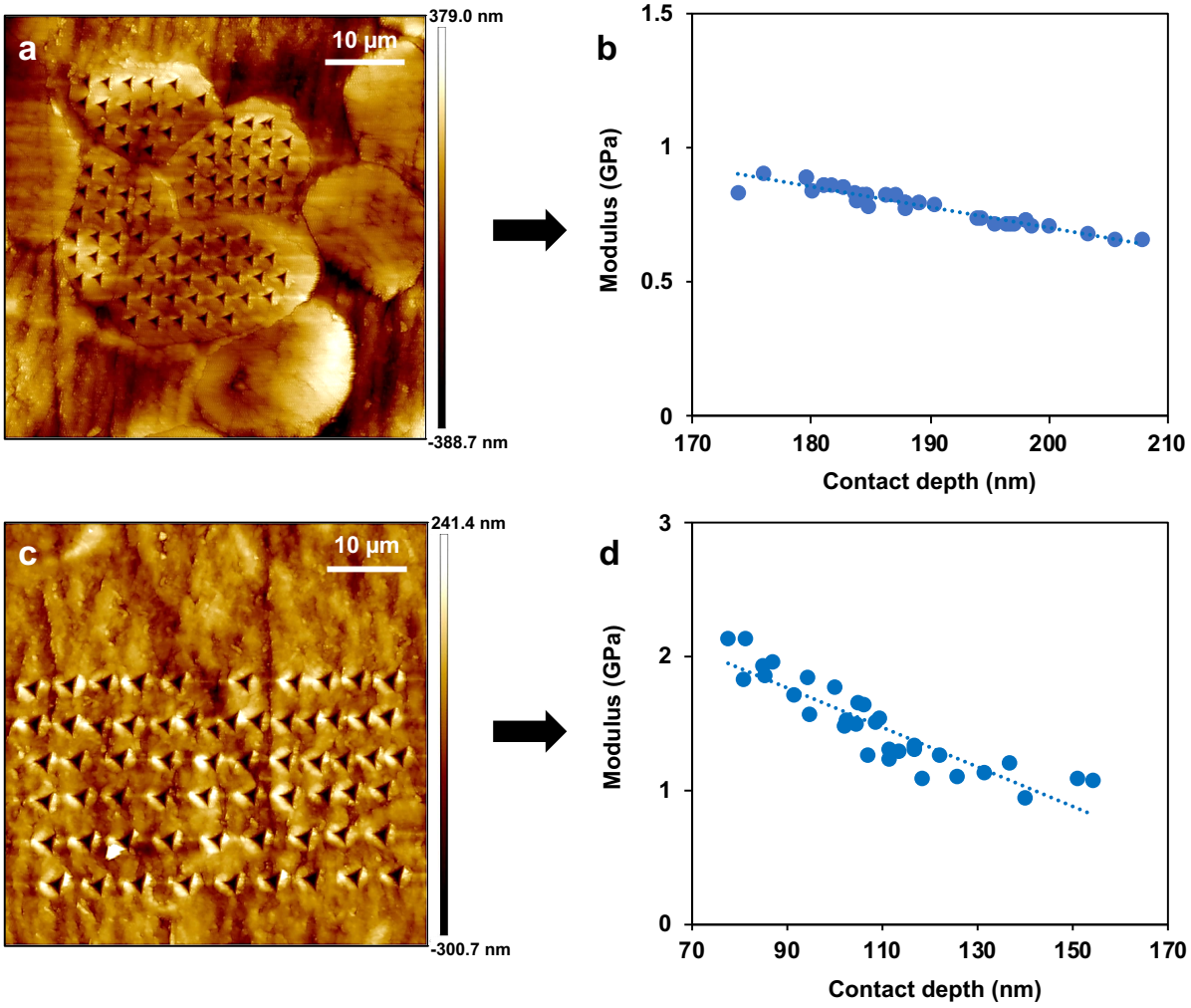

Figure 5: (a) AFM scanning image of indented flax fibers. (b) Elastic modulus of flax fibers obtained by AFM nanoindentation. (a) AFM scanning image of indented PP matrix. (c) Elastic modulus of PP matrix obtained by AFM nanoindentation

To increase the geometrical contact scale, Figure 6 shows the elastic modulus values obtained by nanoindentation using the RPM technique with the Hysitron TI-950 device (Chegdani et al., 2018b). In this investigation, a higher tip indenter radius than that of AFM has been used (r = 100 nm) and am applied load range from 100 µN to 500 µN has been considered to generate a large range of contact depth.

Figure 6(a) reveals a different mechanical response of flax fibers comparing to that of AFM indentation of Figure 5(b). Indeed, Figure 6(a) shows an elastic modulus of flax fibers between 5 GPa and 22 GPa for a contact depth range from 25 nm to 230 nm.

These elastic modulus values are largely higher than that obtained by AFM indentation. On the other hand, the mechanical response of PP matrix shown in Figure 6(b) is not significantly different from that of AFM nanoindentation method shown in Figure 5(d) at the same contact depth range. With a tip indenter radius of 100 nm, the elastic modulus of flax fibers becomes higher than that of PP matrix.

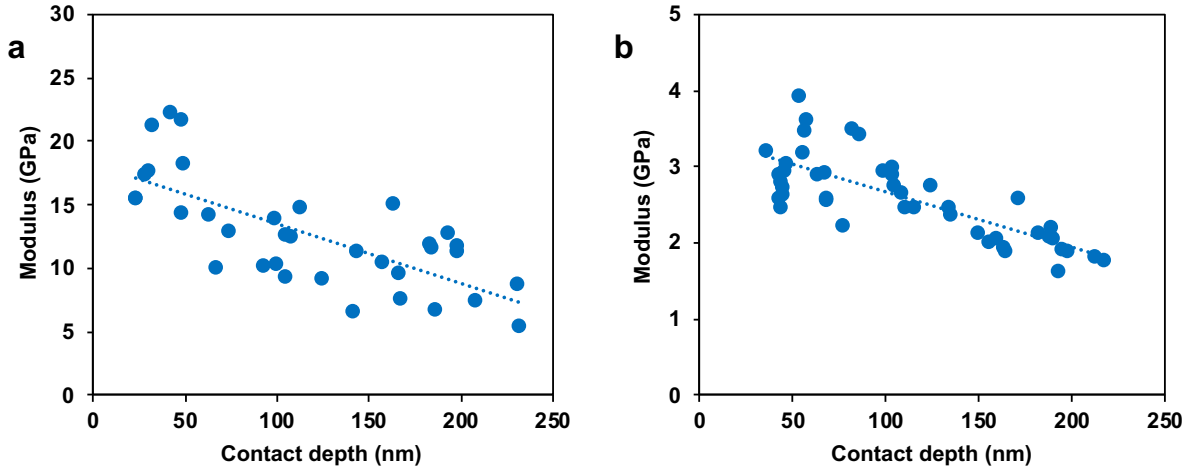

Figure 6: (a) Elastic modulus of flax fibers obtained by RPM nanoindentation. (b) Elastic modulus of PP matrix obtained by RPM nanoindentation

The investigation of the tip indenter radius (r) effect has been performed also with r = 150 nm (Chegdani et al., 2019) and r = 400 nm (Chegdani et al., 2017). Figure 7 gives a comparison of the elastic modulus obtained with the different tip indenter radii for flax fibers and PP matrix for the same applied load (F_{max} = 500 µN).

The elastic modulus of flax fibers shows a significant increase when increasing the tip indenter radius, while the elastic modulus of PP matrix remains almost constant. This demonstrates the scale effect on the mechanical response of flax fiber induced by the geometrical contact scale. The multiscale mechanical behavior of flax fibers shown in this study is strongly related to the multiscale cellulosic structure of natural fibers (microfibrils → mesofibrils → elementary fibers) that affects the nature of the mechanical contact during the indentation. Indeed, when indenting with low tip indenter radius below the mesofibrils diameter (100 – 300 nm) (Bos et al., 2004), the cellulose

microfibrils (diameters between 1 – 4 nm (Bos et al., 2004)) are transversally deviated from the indentation path as shown in Figure 7(a). The mechanical response is almost that of non-cellulosic polymers in contact with the tip indenter. Since the tip intender radius reaches the mesofibrils size, the indentation contact interface will include also the microfibrils that have high stiffness (135 GPa (Baley, 2002)) as shown in Figure 7(b). Therefore, the indentation modulus increases by increasing the microfibrils contents in the contact area.

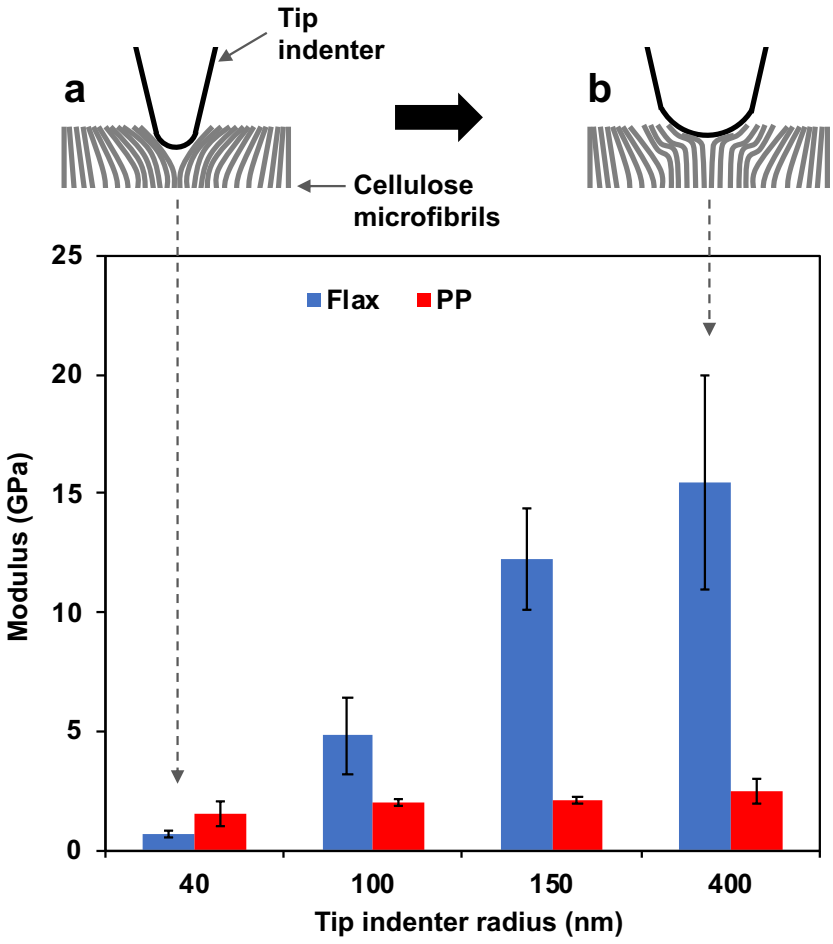

Figure 7: Elastic modulus of flax fibers and PP matrix obtained with different tip indenter radii. (a) Schematic illustration of fiber/indenter contact with low indenter radius. (b) Schematic illustration of fiber/indenter contact with high indenter radius

4.2. Multiscale frictional response of natural fiber composites

The frictional response of NFC has been investigated by calculating the dynamic friction coefficient (μ_D) obtained from scratch-test experiments as the ratio between the scratching force (friction force) and the applied load (normal force). Scratch-test experiments were performed with AMF technique and RPM method by the Hisytron TI-950 device. Scratch-test experiments with AFM technique are not performed with the similar loading scale as for the RPM device. Indeed, lateral scratching motions with AFM indenters cannot be performed with high loads. Therefore, AFM scratch-tests were limited to an applied load of 30 µN. For the Hisytron TI-950 devise, scratching experiments were performed with the Diamond indenter (r = 100 nm) and Sapphire indenter (r = 150 nm) with an applied load of 500 µN. Figure 8 shows the typical scratching traces performed by RPM indenter. It can be seen that scratching traces of flax fibers and PP matrix have not the same shape. Plowed material is clearly observed at the bordered of each groove on PP matrix (Figure 8 (b)). For flax fibers, the grooves are formed without any noticeable plowing (Figure 8(a)). The difference in the scratching mechanisms that occurs on flax fibers and PP matrix can be due to the high plasticity of PP matrix compared to flax fibers as shown in the nanoindentation study reported in section 4.1.

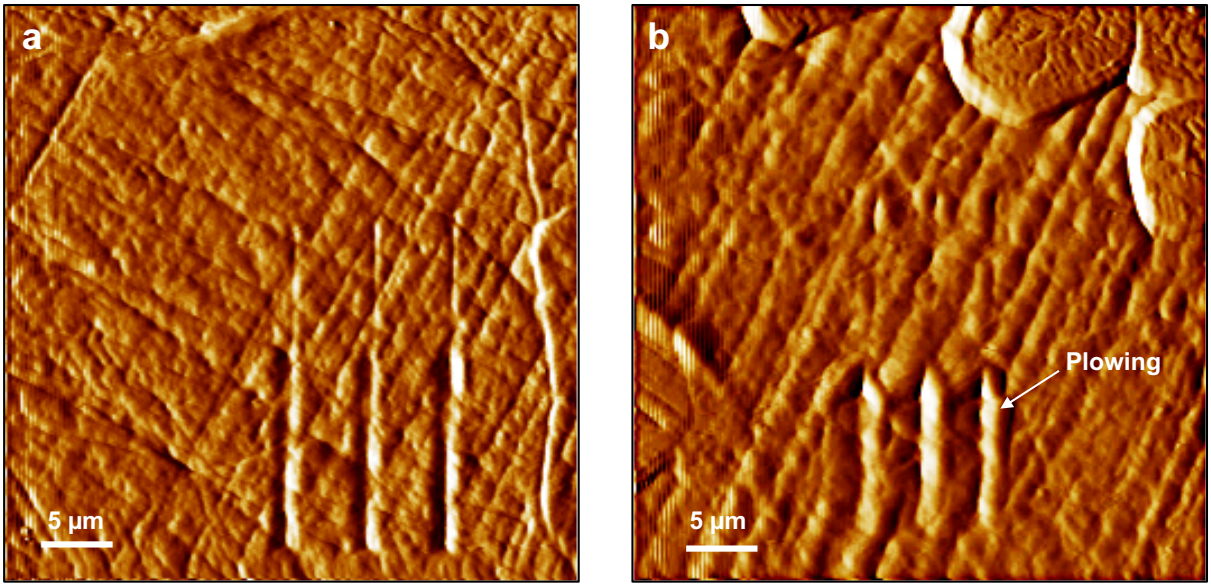

Figure 8: Scratching grooves performed with RPM device using Diamond indenter at 500 µN of applied load on (a) flax fibers and (b) PP matrix

Figure 9 shows the dynamic friction coefficient (μ_D) generated by scratch-test experiments with AFM and RPM techniques. The first obvious observation is that AFM scratching friction coefficient (Figure 9(a)) is not on the same order of magnitude than that of RPM scratching (Figure 9(b)). Moreover, the friction coefficient of PP matrix is higher than that of flax fibers during the AFM scratching. However, the trend is reversed for the RPM scratching where the friction coefficient of flax fibers is higher than that of PP matrix. The raisons behind this difference could be related to both the contact and the load scales. Indeed, two scratching parameters are different between the two methods:

- The applied load: 30µN for AFM scratching and 500 µN for RPM scratching
- The tip indenter radius: 40 nm for AFM scratching and 100 nm for RPM scratching

The variation of these two parameters affects the friction mechanisms. As well known, friction is a complex phenomenon that cannot be reduced to a single mechanism, but rather a result of a simultaneous action of various mechanisms at different hierarchy and scale levels such as adhesion, shear, and plowing (Chegdani and El Mansori, 2018; Nosonovsky and Bhushan, 2007). At low applied loads (30 µN), the predominant

friction mechanism is adhesion that has an important role at nanoscale by controlling the interaction forces between the atoms of the two surfaces in contact (Nosonovsky and Bhushan, 2007). This explain the low values of friction coefficient obtained with AFM scratching (Figure 9(a)). Changing the loading scale (30 μN → 500 μN) leads to the inclusion of further friction mechanisms such us shearing and plowing due to the increase of the contact depth of scratching. The friction coefficient is then upgraded to another scale level as shown in Figure 9(b) for RPM scratching.

The frictional responses of flax fibers and PP matrix are also affected by the geometrical contact scale that controls the mechanical response as shown with nanoindentation experiments in section 4.1. Indeed, the geometrical contact with an indenter radius of 40 nm engenders an elastic modulus of PP matrix higher than that of flax fibers. Consequently, the tangential scratching force of PP matrix is higher than that of flax fibers which is reflected on the friction coefficient results of Figure 9(a). When upgrading the contact scale to 100 nm, the cellulose microfibrils come into play and increase the tangential scratching force of flax fibers which makes the friction coefficient of flax fibers higher than that of PP matrix as shown in Figure 9(b).

On the other hand, the difference of RPM scratching friction between Diamond tip indenter (Figure 9(b)) and Sapphire tip indenter(Figure 9(c)) is mainly due to the effect of the tip material that lead to change the frictional properties between the tip and the worksurface.

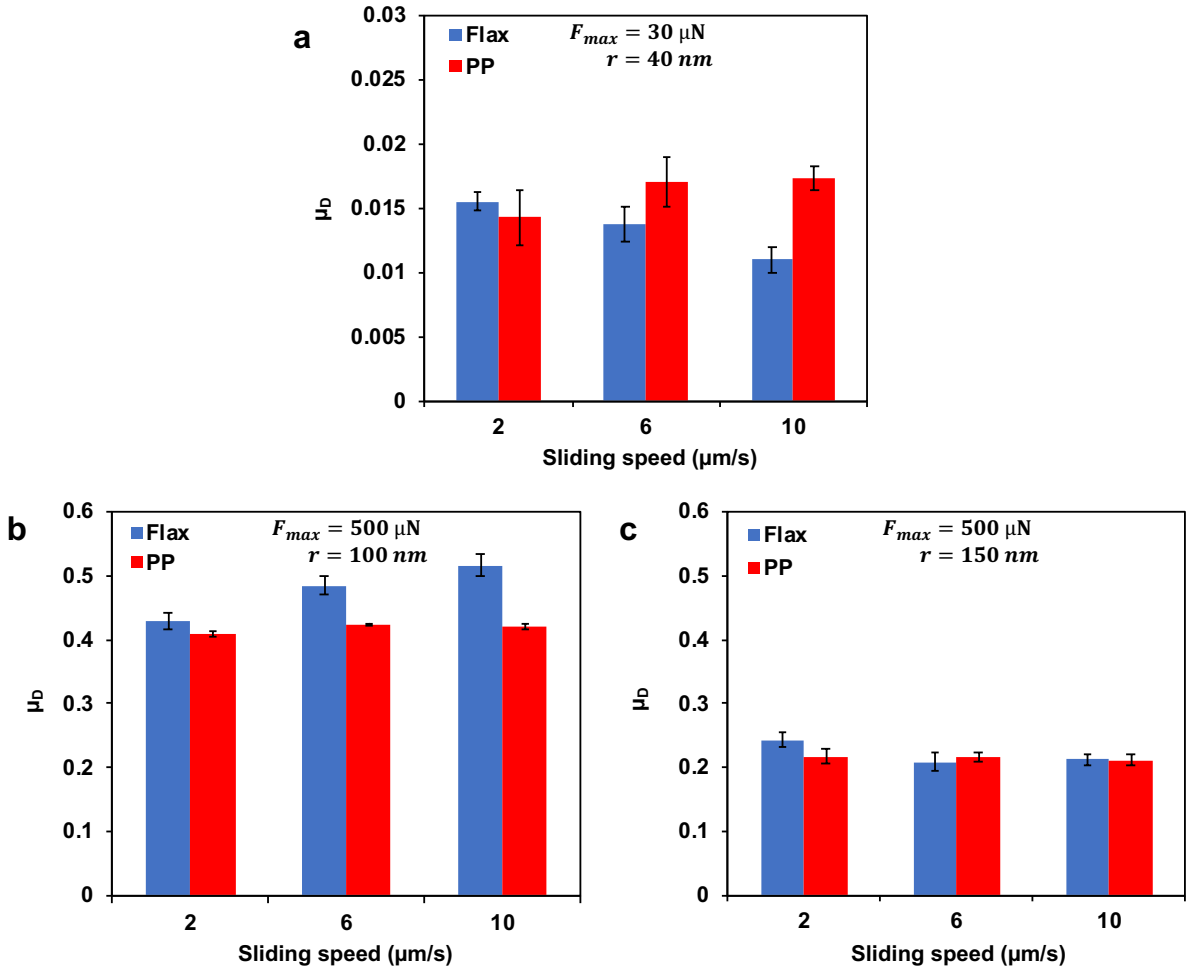

Figure 9: Friction coefficient obtained by scratch-test with (a) AFM technique and diamond tip indenter, (b) RPM technique and diamond tip indenter, and (c) RPM technique and Sapphire tip indenter.

5. Thermal effect on the tribo-mechanical response of natural fiber composites

5.1. Thermomechanical response of natural fiber composites

The effect of sample temperature on the mechanical response of flax fibers and PP matrix has been performed with RPM nanoindentation technique using the Sapphire tip indenter (Chegdani et al., 2019). A large sample temperature range has been considered from room temperature (25 ºC) to 100 ºC. Figure 10 presents the evolution of the elastic modulus in function of sample temperature at iso applied load (500 µN) for flax fibers and PP matrix. Figure 10(b) shows that increasing the sample temperature decreases significantly the stiffness of PP matrix. This reveals that the sample temperature affects strongly the softening of PP matrix. This thermo-mechanical behavior is well known in the literature for thermoplastic polymers (Drozdov, 2010; Tripathi, 2002). Thermoplastic matrices soften under the effect of heat and become malleable at high temperatures with a significant decrease of the viscosity (Kannan et al., 2013).

On the other side, the thermal effect on flax fibers is completely different as shown in Figure 10(a). Indeed, in the temperature range of [25 - 60 °C], the elastic modulus of flax fibers increases by temperature increase. However, in the temperature range of [60 - 100 °C], the elastic modulus of flax fibers decreases by temperature increase. This specific behavior of flax fibers under thermal nanoindentation may be due to the chemical composition of their cellulosic structure shown in section 2. Indeed, the cellulosic composition of natural fibers provides them a hydrophilic character that gives each elementary fiber the ability to absorb water molecules from the environment (Dittenber and GangaRao, 2012). Therefore, when indenting flax fibers from 25°C to

60°C, increasing the sample temperature leads to water release that acts as a plasticizer into the fiber structure (N.-S. Hon and Shiraishi, 2000). This thermal effect on moisture content of flax fibers can explain the stiffness increase when heating flax fibers in the temperature range [25°C – 60°C]. Above 60°C, glass transition temperatures of the amorphous polymers inside the flax fiber are reached which makes the fiber softer. In fact, the glass transition temperature is 40 °C for hemicelluloses, 50 °C to 100 °C for lignin, and above 100 °C for cellulose (Kong et al., 2017). Therefore, increasing the temperature above 60°C leads to exceeding the glass transition temperature of hemicellulose which is responsible of the bonding of cellulose microfibrils (Pere et al., 2019). Consequently, the rigidity of fiber decreases when heating flax fibers in the temperature range [60°C – 100°C].

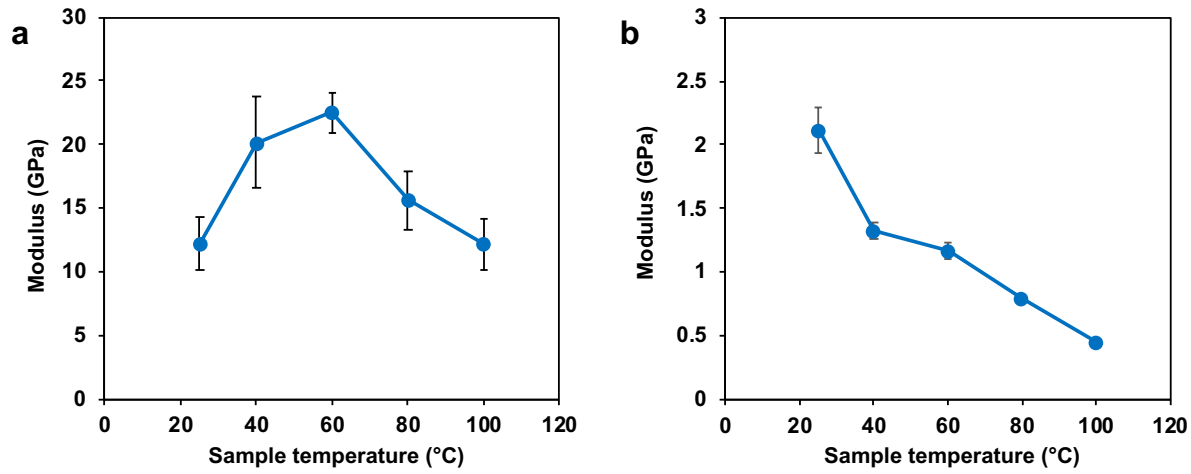

Figure 10: Elastic modulus obtained by RPM nanoindentation at different sample temperatures for (a) flax fibers, and (b) PP matrix

5.2. Thermo-frictional response of natural fiber composites

Thermo-frictional analysis of NFC has been performed with scratch-test using the same experimental setup described in Section 5.1 to reveal the effect of sample temperature. Figure 11 presents the friction coefficient of flax fibers and PP matrix at different sample temperatures. The friction coefficient of PP matrix decreases by

increasing the sample temperature. This frictional behavior at microscale is in good agreement with its mechanical response shown in Figure 10(b) and also with the sliding friction of PP reported in literature at macroscale by standard tribometers where the sliding friction of PP polymer decreases with temperature increase (Ludema and Tabor, 1966). This is due to the polymer softening that leads to the decrease of the tangential scratching force (Chegdani et al., 2019).

The frictional response of flax fibers shows a specific behavior that is similar to their mechanical behavior presented in section 5.1. Indeed, the friction coefficient of flax fibers increases by increasing the sample temperature from 25 °C to 60 °C and decreases by heating the samples even further from 60 °C to 100 °C as shown in Figure 11. This demonstrated once again the local functional relationship between the mechanical response and the frictional response of each composite component. As for PP matrix, increasing the rigidity of flax fibers increases their tangential scratching force which contributes to a rise of the friction coefficient.

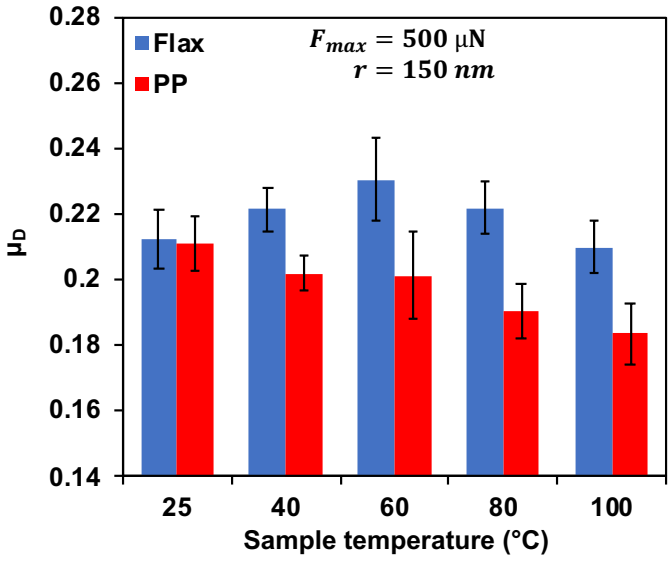

Figure 11: Friction coefficient obtained by RPM scratch-test for flax fibers and PP matrix.

6. Conclusions

In this chapter, the tribo-mechanical behavior of natural fiber composites (NFC) has been investigated by performing nanoindentation and scratch-test experiments on flax fiber reinforced polypropylene matrix at different scale levels. The following conclusions can be drawn:

- Unlike PP matrix, the elastic modulus of flax fibers shows a tough dependence on the geometric contact scale where increasing the indenter tip radius increases significantly the fiber stiffness. Therefore, flax fibers engender multiscale mechanical properties that are related to their multiscale cellulosic structure.
- The local friction behavior of flax fibers and PP matrix shows a strong functional relationship with their respective local mechanical properties.
- The mechanical properties of NFC show a significant thermal effect that differs from flax fibers to the PP matrix. The thermal effect on mechanical properties is thus transposed to the frictional behavior of flax fibers and PP matrix.

7. References

Baley, C., 2002. Analysis of the flax fibres tensile behaviour and analysis of the tensile stiffness increase. Compos. - Part A Appl. Sci. Manuf. 33, 939–948. https://doi.org/10.1016/S1359-835X(02)00040-4

Bos, H.L., Molenveld, K., Teunissen, W., van Wingerde, A.M., van Delft, D.R. V, 2004. Compressive behaviour of unidirectional flax fibre reinforced composites. J. Mater. Sci. 39, 2159–2168. https://doi.org/10.1023/B:JMSC.0000017779.08041.49

Bos, H.L., Müssig, J., van den Oever, M.J.A., 2006. Mechanical properties of short-

flax-fibre reinforced compounds. Compos. Part A Appl. Sci. Manuf. 37, 1591–1604. https://doi.org/10.1016/J.COMPOSITESA.2005.10.011

Bourmaud, A., Pimbert, S., 2008. Investigations on mechanical properties of poly(propylene) and poly(lactic acid) reinforced by miscanthus fibers. Compos. Part A Appl. Sci. Manuf. 39, 1444–1454. https://doi.org/10.1016/j.compositesa.2008.05.023

Charlet, K., Baley, C., Morvan, C., Jernot, J.P., Gomina, M., Bréard, J., 2007. Characteristics of Hermès flax fibres as a function of their location in the stem and properties of the derived unidirectional composites. Compos. Part A Appl. Sci. Manuf. 38, 1912–1921. https://doi.org/10.1016/j.compositesa.2007.03.006

Chegdani, F., El Mansori, M., 2019. Tribo-functional effects of double-crossed helix on surface finish, cutting friction and tool wear mechanisms during the milling process of natural fiber composites. Wear 426–427, 1507–1514. https://doi.org/10.1016/j.wear.2018.11.026

Chegdani, F., El Mansori, M., 2018. Friction scale effect in drilling natural fiber composites. Tribol. Int. 119, 622–630. https://doi.org/10.1016/j.triboint.2017.12.006

Chegdani, F., El Mansori, M., Bukkapatnam, S.T.S., El Amri, I., 2019. Thermal effect on the tribo-mechanical behavior of natural fiber composites at micro-scale. Tribol. Int. https://doi.org/10.1016/j.triboint.2019.06.024

Chegdani, F., El Mansori, M., Mezghani, S., Montagne, A., 2017. Scale effect on tribo-mechanical behavior of vegetal fibers in reinforced bio-composite materials. Compos. Sci. Technol. 150, 87–94. https://doi.org/10.1016/j.compscitech.2017.07.012

Chegdani, F., Mansori, M. El, 2018. Mechanics of material removal when cutting

natural fiber reinforced thermoplastic composites. Polym. Test. 67, 275–283. https://doi.org/10.1016/j.polymertesting.2018.03.016

Chegdani, F., Mezghani, S., El Mansori, M., 2016. On the multiscale tribological signatures of the tool helix angle in profile milling of woven flax fiber composites. Tribol. Int. 100, 132–140. https://doi.org/10.1016/j.triboint.2015.12.014

Chegdani, Faissal, Mezghani, S., El Mansori, M., 2015. Experimental study of coated tools effects in dry cutting of natural fiber reinforced plastics. Surf. Coatings Technol. 284, 264–272. https://doi.org/10.1016/j.surfcoat.2015.06.083

Chegdani, F., Mezghani, S., El Mansori, M., Mkaddem, A., 2015. Fiber type effect on tribological behavior when cutting natural fiber reinforced plastics. Wear 332–333, 772–779. https://doi.org/10.1016/j.wear.2014.12.039

Chegdani, F., Takabi, B., Tai, B.L., Mansori, M. El, Bukkapatnam, S.T.S., 2018a. Thermal Effects on Tribological Behavior in Machining Natural Fiber Composites. Procedia Manuf. 26, 305–316. https://doi.org/10.1016/j.promfg.2018.07.039

Chegdani, F., Wang, Z., El Mansori, M., Bukkapatnam, S.T.S., 2018b. Multiscale tribo-mechanical analysis of natural fiber composites for manufacturing applications. Tribol. Int. 122, 143–150. https://doi.org/10.1016/j.triboint.2018.02.030

Dittenber, D.B., GangaRao, H.V.S., 2012. Critical review of recent publications on use of natural composites in infrastructure. Compos. Part A Appl. Sci. Manuf. https://doi.org/10.1016/j.compositesa.2011.11.019

Doerner, M.F., Nix, W.D., 1986. A method for interpreting the data from depth-sensing indentation instruments. J. Mater. Res. 1, 601–609. https://doi.org/https://doi.org/10.1557/JMR.1986.0601

Drozdov, A.D., 2010. Effect of temperature on the viscoelastic and viscoplastic behavior of polypropylene. Mech. Time-Dependent Mater. 14, 411–434. https://doi.org/10.1007/s11043-010-9118-5

Faruk, O., Bledzki, A.K., Fink, H.-P., Sain, M., 2012. Biocomposites reinforced with natural fibers: 2000–2010. Prog. Polym. Sci. 37, 1552–1596. https://doi.org/10.1016/j.progpolymsci.2012.04.003

Goutianos, S., Peijs, T., Nystrom, B., Skrifvars, M., 2006. Development of Flax Fibre based Textile Reinforcements for Composite Applications. Appl. Compos. Mater. 13, 199–215. https://doi.org/10.1007/s10443-006-9010-2

Jiang, L., Walczyk, D., McIntyre, G., Bucinell, R., Tudryn, G., 2017. Manufacturing of biocomposite sandwich structures using mycelium-bound cores and preforms. J. Manuf. Process. 28, 50–59. https://doi.org/10.1016/J.JMAPRO.2017.04.029

Kannan, T.G., Wu, C.M., Cheng, K.B., Wang, C.Y., 2013. Effect of reinforcement on the mechanical and thermal properties of flax/polypropylene interwoven fabric composites. J. Ind. Text. 42, 417–433. https://doi.org/10.1177/1528083712442695

Kong, L., Zhao, Z., He, Z., Yi, S., 2017. Effects of steaming treatment on crystallinity and glass transition temperature of Eucalyptuses grandis × E. urophylla. Results Phys. 7, 914–919. https://doi.org/10.1016/J.RINP.2017.02.017

Lotfi, A., Li, H., Dao, D.V., Prusty, G., 2019. Natural fiber–reinforced composites: A review on material, manufacturing, and machinability. J. Thermoplast. Compos. Mater. 089270571984454. https://doi.org/10.1177/0892705719844546

Ludema, K.C., Tabor, D., 1966. The friction and visco-elastic properties of polymeric solids. Wear 9, 329–348. https://doi.org/10.1016/0043-1648(66)90018-4

Marrot, L., Lefeuvre, A., Pontoire, B., Bourmaud, A., Baley, C., 2013. Analysis of the

hemp fiber mechanical properties and their scattering (Fedora 17). Ind. Crops Prod. 51, 317–327. https://doi.org/10.1016/j.indcrop.2013.09.026

Mastura, M.T., Sapuan, S.M., Mansor, M.R., Nuraini, A.A., 2018. Materials selection of thermoplastic matrices for 'green'' natural fibre composites for automotive anti-roll bar with particular emphasis on the environment.' Int. J. Precis. Eng. Manuf. Technol. 5, 111–119. https://doi.org/10.1007/s40684-018-0012-y

Monclus, M.A., Young, T.J., Di Maio, D., 2010. AFM indentation method used for elastic modulus characterization of interfaces and thin layers. J. Mater. Sci. 45, 3190–3197. https://doi.org/10.1007/s10853-010-4326-6

N.-S. Hon, D., Shiraishi, N., 2000. Wood and Cellulosic Chemistry, Marcel Dek. ed. New York.

Nassar, M.M.A., Arunachalam, R., Alzebdeh, K.I., 2017. Machinability of natural fiber reinforced composites: a review. Int. J. Adv. Manuf. Technol. 88, 2985–3004. https://doi.org/10.1007/s00170-016-9010-9

Nosonovsky, M., Bhushan, B., 2007. Multiscale friction mechanisms and hierarchical surfaces in nano- and bio-tribology. Mater. Sci. Eng. R Reports 58, 162–193. https://doi.org/10.1016/J.MSER.2007.09.001

Oliver, W.C., Pharr, G.M., 1992. An Improved Technique for Determining Hardness and Elastic-Modulus Using Load and Displacement Sensing Indentation Experiments. J. Mater. Res. 7, 1564–1583. https://doi.org/10.1557/

Pere, J., Pääkkönen, E., Ji, Y., Retulainen, E., 2019. Influence of the hemicellulose content on the fiber properties, strength, and formability of handsheets. BioResources 14, 251–263. https://doi.org/10.15376/biores.14.1.251-263

Rajmohan, T., Vinayagamoorthy, R., Mohan, K., 2019. Review on effect machining parameters on performance of natural fibre–reinforced composites (NFRCs). J.

Thermoplast. Compos. Mater. 32, 1282–1302. https://doi.org/10.1177/0892705718796541

Ramesh, M., Palanikumar, K., Hemachandra Reddy, K., 2017. Plant fibre based bio-composites: Sustainable and renewable green materials. Renew. Sustain. Energy Rev. 79, 558–584. https://doi.org/10.1016/J.RSER.2017.05.094

Roy Choudhury, M., Srinivas, M.S., Debnath, K., 2018. Experimental investigations on drilling of lignocellulosic fiber reinforced composite laminates. J. Manuf. Process. 34, 51–61. https://doi.org/10.1016/J.JMAPRO.2018.05.032

Shah, D.U., 2013. Developing plant fibre composites for structural applications by optimising composite parameters: a critical review. J. Mater. Sci. 48, 6083–6107. https://doi.org/10.1007/s10853-013-7458-7

Shalwan, A., Yousif, B.F., 2013. In State of Art: Mechanical and tribological behaviour of polymeric composites based on natural fibres. Mater. Des. 48, 14–24. https://doi.org/10.1016/j.matdes.2012.07.014

Tripathi, D., 2002. Practical Guide to Polypropylene, Rapra Tech. ed. Shropshire.

Vinayagamoorthy, R., Rajmohan, T., 2018. Machining and its challenges on bio-fibre reinforced plastics: A critical review. J. Reinf. Plast. Compos. 37, 1037–1050. https://doi.org/10.1177/0731684418778356

Yan, L., Chouw, N., Jayaraman, K., 2014. Flax fibre and its composites – A review. Compos. Part B Eng. 56, 296–317. https://doi.org/10.1016/J.COMPOSITESB.2013.08.014